THEORETICAL STUDIES OF ELECTRICAL CHARACTERISTICS OF THE NITROGEN LASER

H. Golnabi and A. Ashrafi

Institute of Water and Energy
Sharif University of Technology
Tehran, Iran

Abstract A theoretical analysis of the circuits for a nitrogen laser driven by the Blumlein or capacitor charge transfer transmission line is given in detail. The electrical characteristics of the charge line for a special case of resonant charging are discussed and the effects of various parameters on voltage and current are investigated. By using MICRO-CAP software the transient behavior of the current and voltage in both the charge and discharge processes are studied and an optimum situation for a better laser performance is reported. The theoretical results obtained here could provide insights into the design and construction of high power gas lasers.

Key Words Electrical Characteristics, Nitrogen Laser, Electrical Excitation, Charge, Discharge, Blumlein Circuit

چکیده در این مقاله یک بررسی نظری کامل از مدار الکتریکی لیزر ازت تحریک شده به وسیله خط انتقال بولملین (Blumlein) و یا خازن به خازن، انجام گرفته است. خصوصیات الکتریکی مربوط به حالت خاص شارژ تشدیدی توصیف شده، و اثر هریک از پارامترهای مدار بر روی ولتاژ و جریان شارژ بررسی شده اند. با استفاده از نرم افزار میکروکپ (MICROCAP) رفتارگذرای مربوط به ولتاژ و جریان دشارژ برای هردو نوع خط انتقال لیزر تحلیل شده اند و با استفاده از نتایج بدست آمده شرایط بهینه برای عملکرد هر لیزر گزارش شده اند. با مقایسه اطلاعات به دست آمده با نتایج عملی در این راستا، کارایی روش نظری برای تحلیل مدار الکتریکی لیزر ازت نشان داده شده است. نتایج مطالعات انجام شده نشان می دهند که روش ارائه شده می تواند به خوبی برای طراحی مدارهای الکتریکی لیزرهای پرقدرت گازی دیگر نیز مورد استفاده قرار گیرد.

INTRODUCTION

The superradiant laser action in nitrogen gas occurring at 337.1 nm was discovered by Heard [1] in 1963, and since then several investigation of the gas in the 10-20 ns range have been developed to obtain a uniform glow discharge in nitrogen gas at low pressures (20-100 Torr). Still faster excitation methods have been developed for achieving a higher laser power in transversely excited atmospheric-pressure (TEA) nitrogen laser [3,4]. Different studies have dealt with the various aspects of the physical parameters associated with the formation of a discharge pulse in a nitrogen plasma tube. However, the knowlede of accurate information concerning the electrical resonant charge and discharge processes is limited to a few cases [5,6]. Therefore, a precise analysis may have many applications in the design, development, and construction of such a molecular gas laser.

A new theoretical model for the analysis of the resonant charging process in a Blumlein driven nitrogen laser was detailed in the previous paper [7]. This paper reports on the use of a resonant charging mechanism and a fast excitation for the discharge process. Here, we report the theoretical studies of the electcical charge and discharge operation in both the Blumlein and capacitor charge transfer transmission lines, and information on the voltage and current behavior that can be derived from such calculations. The results show that this type of theoretical approach and calculations could be applicable to the design and construction of high-power discharges in many other gas lasers such as excimers [8].

ELECTRICAL CHARACTERISTICS

When nitrogen laser is electrically excited, the required fast current rise time puts severe restrictions on the inductances and impedances of the discharge circuit. Transmission lines are often used for energy storage and for the coupling of the electrical energy to the laser electrodes in order to produce a high population inversion density in the plasma tube. A switching means is also provided to allow the line to be charged up to the desired voltage before the gas breakdown occurs in the main discharge chamber [9].

The overall circuitry of the system discussed here consists of the power supply and the laser circuit. The layout of the power supply is elaborated in Reference 7. In the majority of transversely excited nitrogen lasers, a Blumlein circuit is used as an efficient discharge circuit to produce a fast rising discharge. A minor variation of the Blumlein circuit is the so called capacitor-to-capacitor charge transfer circuit (C-C). Both of the circuits consist of an energy storage capacitor, a pulse forming line, a triggering switch and a laser discharge channel. The main difference is in the placement of the triggering switch and the laser plasma chamber in the circuits [10].

The circuits shown in Figure1 (a) and 1 (b) are used to model the electrical characteristics of the nitrogen laser head. The parallel plate capacitors are considered for both types of the Blumlein and capacitor charge trarsfer transmission lines which have a typical impedance of about 0.15Ω. The C-C circuit shown in Figure 1 (a) includes the storage capacitors C1 and C2, charging resistor, R, laser tube electrodes and the spark gap which is used for triggering the line. Figure 1 (b) shows the Blumlein line circuit which is assumed to be constructed from similar components in a different arrangement.

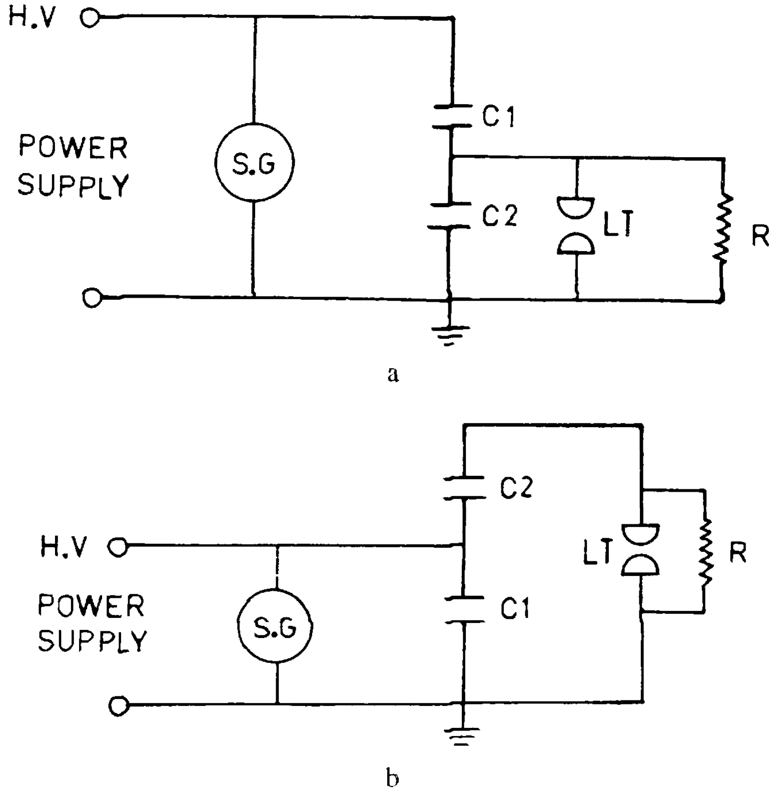

Figure 1. Typical excitation circuits **(a)** the (C-C) pulse generator **(b)** the Blumlein circuit. In both figures the spark gap switch is indicated by S. G, and the laser tube discharge is shown by LT.

CHARGE AND DISCHARGE CIRCUITS

A theoretical model which treated the laser power supply circuit and storage capacitors as an integrated system was described and a general form for the voltage and current pulses were reported in a previous work [7]. Following the procedure given in that report, the simplified equivalent circuit for the charging process in a Blumlein circuit is reproduced in Figure 2. The parameters involved in the charge cycle are R, C, Lp and the variable inductor L. With the proper value of the inductor L in the primary of the transformer, the best condition can be obtained when the charge voltage reaches its peak value and the current passes through zero simultaneously.

A similar equivalent circuit can be drawn for the C-C drive circuit where the value of the storage capacitor which transforms into the primary is different from that of the Blumlein circuit. However, the analysis is the same for both lines, and by using the MICRO-CAP program the charge voltage, current,

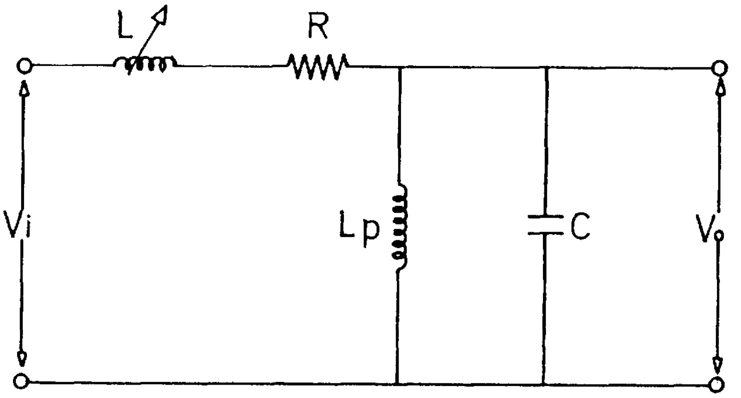

Figure 2. Drive circuit used for modeling the charging system of the laser at resonant condition.

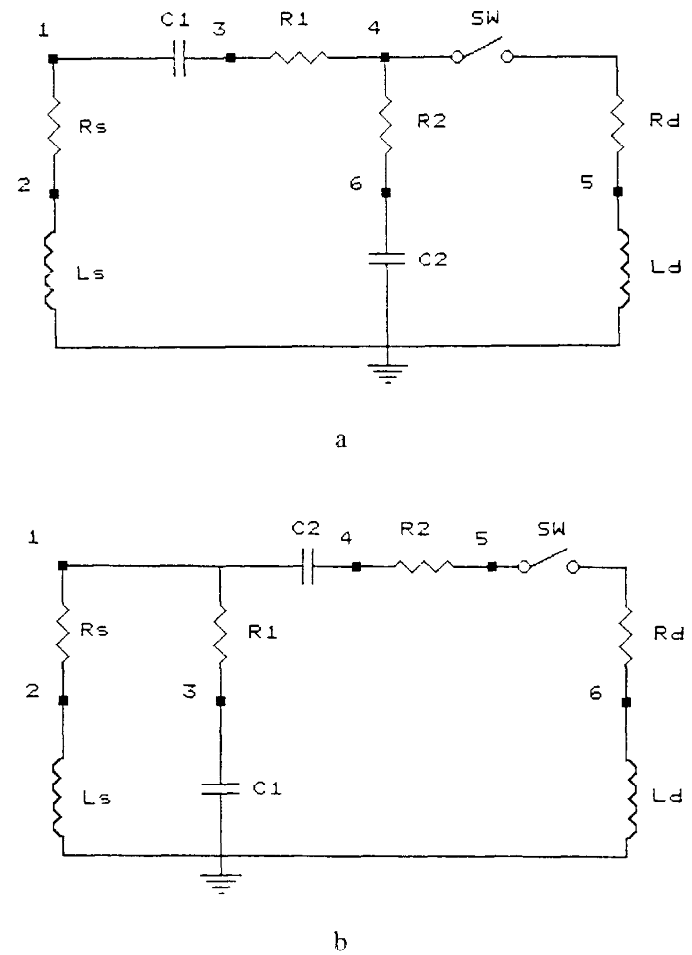

Figure 3. Equivalent circuits **(a)** the C-C circuit, **(b)** Blumlein line. The spark gap is replaced by the resistor Rs and the inductor Ls, whereas Rd and Ld represent the laser main discharge tube. The intrinsic resistances (R1 and R2) are considered for the capacitors C1 and C2, respectively.

and their correlations are investigated in detail.

To analyze the discharge process, the equivalent circuits for the excitation are shown in Figure 3 (a) and 3 (b) for the C-C and Blumlein lines, respectively. Since gas molecules act as a time-dependent resistance, the spark gap and laser plasma tube are considered as a resistor in a series with a characteristic inductor. The electric circuit shown in Figure 3 (a) consists of the left and right loop, whereas the spark gap closes the left loop, and the laser plasma tube closes the right loop during the discharge operation. The primary energy storage is contained in capacitor C1, and due to the charging resistor the energy on the capacitor C2 is very small at the initial discharge process. After the spark gap closes, the initial current passes through the spark gap and in the left loop a lumped RLC circuit exists which oscillates at a high frequency. Because of the initial current flow, a potential difference begins to form across the laser tube. After some time elapse, the main discharge is initiated by closing the tube conducting gas in the right loop circuit.

The analysis of the network shown in Figure 3 (b) for the Blumlein transmission line is straightforward, and a similar argument for the lumped RLC circuit can be made as well. The discharge sequence begins with the application of an initial voltage pulse, and in the rising part of the first cycle the nitrogen gas in the spark gap is assumed to break down, hence the current flowing through the resistor and inductor represents the spark gap switch. After a suitable time delay, the main laser discharge is initiated by closing the right loop circuit.

RESULTS AND DISCUSSIONS

Charging Analysis

Computational analysis for the charging procedure performed by defining the equivalent circuit is shown in Figure 2 for the MICRO-CAP software. A sinusoidal input voltage of a peak amplitude of 311V is assumed for the circuit and charge voltage and current time behaviors are investigated for both of the transmission lines. First, the charge voltage characteristic of the Blumlein line for typical values [6] of C1 = C2 = 45 nF, Lp = 10H, R = 0.054 Ω, f =

50 Hz, and the transformer gain of 136 are studied. To check the role of the inductor value, L, in the voltage variation, the analysis is carried out for L = 4 to 32 mH in a 4 mH increment, while other parameters are kept uncharged. The computational results obtained from this analysis for the charge voltage are very similar to those of previous work [7], whereas the voltage peak values show a decrease with an increase in the L values. Another feature of these results is that as the inductor value increases the maximum value of the voltage curve occurs at a later time and the voltage pulsewidth shows an increase of higher L values.

The current analysis of the Blumlein line for the mentioned parameteric values is achieved by using the same software. The charge current time behavior for L = 4 to 32 mH is computed for 20 ms time interval. The trend of current changes for different selected L values is very similar to those of the voltage variation with the exception that the current pulse shapes are somewhat more symmetrical and the rise and fall times are less than those of the related voltage pulses.

The optimum charge condition is when the spark gap fires at the maximum charging voltage and the voltage across the transformer primary goes to zero. One can then assume that the laser discharge circuit is totally independent of the power supply circuit. To obtain this condition, a comparison between the results for the voltage and current is made for different inductor values. From this comparison, the appropriate value of L = 7 mH is found to be the right value for inductor setting (charge voltage is maximum while current is zero), hence the related voltage and current variations for this parameter are investigated. In this case the best timing situation is satisfied, whereas the voltage reaches its peak value at 10 ms time interval, the current passes through zero at this moment. The main result of this analysis is that for this value of inductor the charge voltage and current pulses are tuned to the input voltage frequency (50 Hz) which is required for the resonant condition.

A similar analysis is carried out for the C-C excitation line for the same typical values considered for the Blumlein (same power supply, laser tube, spark gap and different storage capacitor). Due to a difference in the value of the transformed storage capacitor into the primary, the effective capacitance value differs here, so expectedly the optimum inductor value should be altered from the above mentioned value. The voltage time behavior is investigated for L = 8 to 32 mH and the results show a similar pattern as for the Blumlein line. The current analysis is performed for the same range of L values and the obtained results are very similar to those of the Blumlein case, with the exception that they have higher peak values. As a result of the voltage and current computations for different L values, the optimum condition is inferred and is displayed in Figure 4. For the value of L = 24 mH the best charging situation is found for the C-C transmission line.

For a better comparison, the corresponding results for the Blumlein circuit obtained here, were compared with those of the previous work [7]. In that report, a theoretical model that treats the laser and power supply circuits as an integrated system was described.

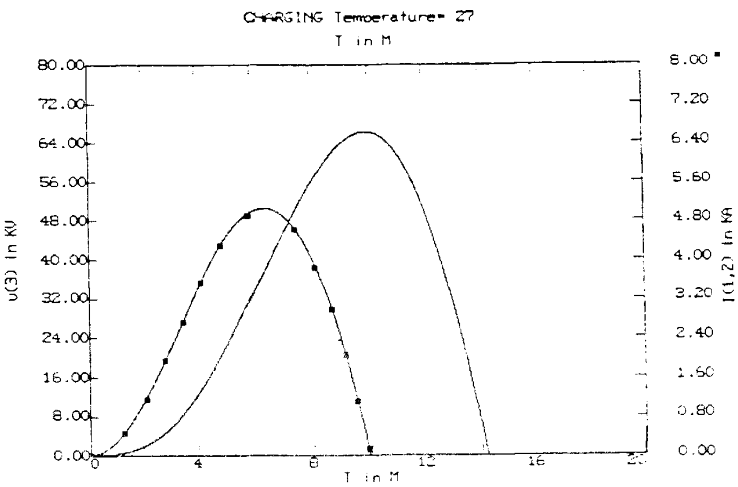

Figure 4. Time history of the charging voltage (solid line) and the current (marked line) for the C-C circuit in the optimum condition. For the value of L=24 mH, while the charge voltage [V_0 = V(3)] is maximum the current, I (1,2), goes through zero at 10 ms time interval.

increased the damping time for current flow also increases. Since the spark gap resistance plays an important role in the discharge operation of the C-C circuit, the transient voltage and current behavior are analyzed for different Rs values. The open-circuit voltage is displayed in Figure 6 which shows the effect of the Rs changes from 0.15 to 0.55 Ω. The obvious result of this study is that for the same Ls value of 3 nH as the spark gap resistance is increased the damping time of the oscillatory motion and its amplitude are decreased, while the Rs variation does not have significant effect on the oscillation frequency. The current flow in the loop as a function of the spark gap resistance is investigated, and the value of Rs is changed from 0.15 to 0.55 Ω. The other important outcome of this analysis is that as the spark gap resistance value is increased the current amplitude and the damping time are decreased, while the oscillation frequency is relatively unchanged.

Similar analysis as those discussed above are carried out for the Blumlein circuit of Figure 3 (b). For the same parametric values, the dependence of the output open - circuit voltage in the case of Ls = 3 to 15 nH is computed and the results are shown in Figure 7. As in the case of the C-C circuit, the amplitude of the ostillations are more pronounced for

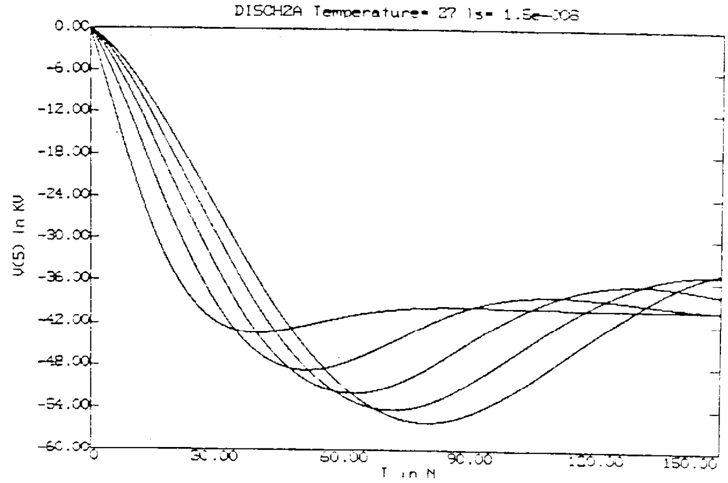

Figure 7. Typical open-circuit output voltage [V (5)] time behavior of the Blumlein circuit for different spark gap inductance, Ls, in 150 ns time interval for applied voltage of 40 kV. Curves from left to right correspond to Ls = 3, 6, 9, 12 and 15 nH, respectively.

the higher Ls values while all voltage curves reach a constant value of about 40 kV at 150 ns time scale. To study the current flow in the circuit for the same range of the Ls variation the current behavior was studied and the results of these computations are plotted in Figure 8.

The effect of the spark gap resistance in the open-circuit voltage and current is also studied in a similar manner and for the same time intervals their behavior is investigated. The results for the voltage time behavior indicate that increasing the Rs value has

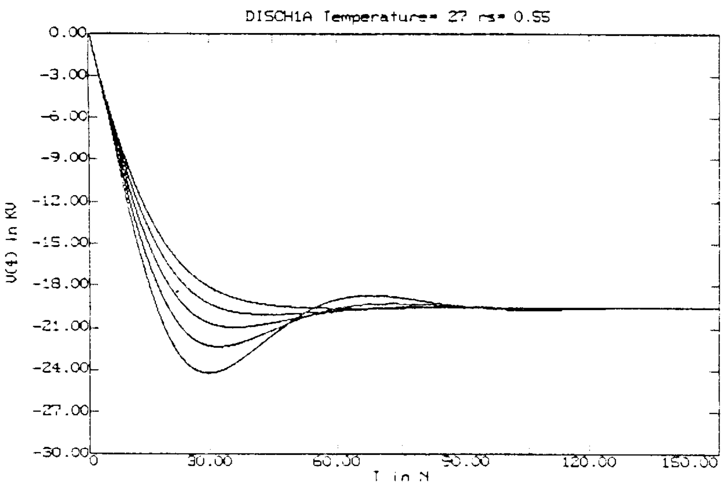

Figure 6. Time history of a typical open-circuit voltage [V(4)] as a function of switch resistance, Rs, for the C-C circuit. Curves from bottom to top present the voltage variation for Rs = 0.15, 0.25, 0.35, 0.45, and 0.55 Ω, respectively.

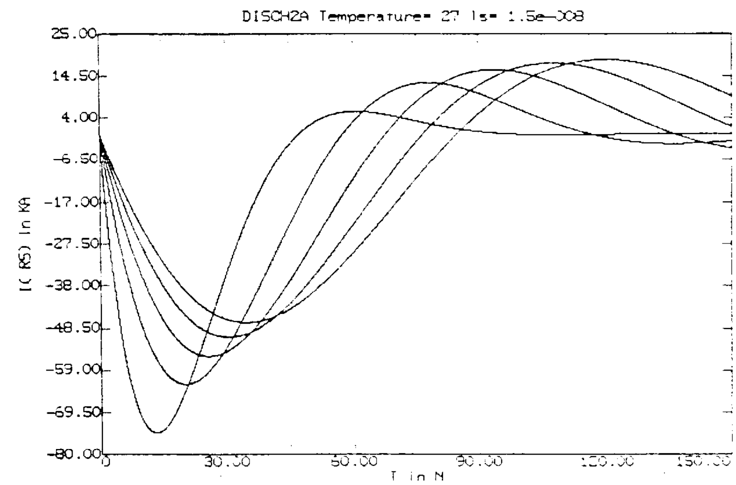

Figure 8. The open-circuit spark gap current [I (Rs)] of Blumlein circuit versus time for different spark gap inductance, Ls. From left to right are curves for Ls = 3, 6, 9, 12, and 15 nH, respectively.

more influence on the amplitude of the oscillation than on the oscillation frequency. The discharge current in this case has an oscillatory behavior which begins at zero, and at a time interval of 15-19 ns (for different Rs values) reaches its maximum, and after a few oscillations at about 150 ns all the current curves reach the zero value again.

In the second part of our analysis discussions of the transient behaviors for the whole discharge circuits shown in Figure 3 (a) and 3 (b) will be presented in detail. This behavior can be quantitatively understood in terms of the LC circuit and the time-dependent impedances of the spark gap and laser discharge tube. The discharge sequence begins with the application of an initial supply voltage across the switch, switch gas breakdown, charging in the left-loop, and in the rising part of the charge voltage the nitrogen gas in the main discharge is assumed to break down and the current flows through the right hand loop. To analyze the discharge process with the software, in order to set the initial values, it is assumed that at the moment that the voltage across the tube reaches 20 kV, the switch will close in order to initiate the discharge operation.

The discharge voltage time variation for the C-C circuit as a function of different laser tube inductance, Ld, from 1 to 9 nH is studied. For the computations it is assumed the other discharge parameters are constant and the Ld dependence is investigated at 150 ns time interval. As the gas breakdown occurs in tube, the load voltage shows the oscillatory behavior whereas the amplitude of oscillation is more obvious for higher Ld values, and the oscillation frequency is decreased in a regular fashion. For the same parameteric values, the main discharge current time variation is considered also, and is shown in Figure 9. The current rise time strongly depends on this parameter as can be seen in the different values of Ld in Figure 9. For a typical value of Ld = 3 nH, the current rise time of the order of 2.8×10^{12} A/s is

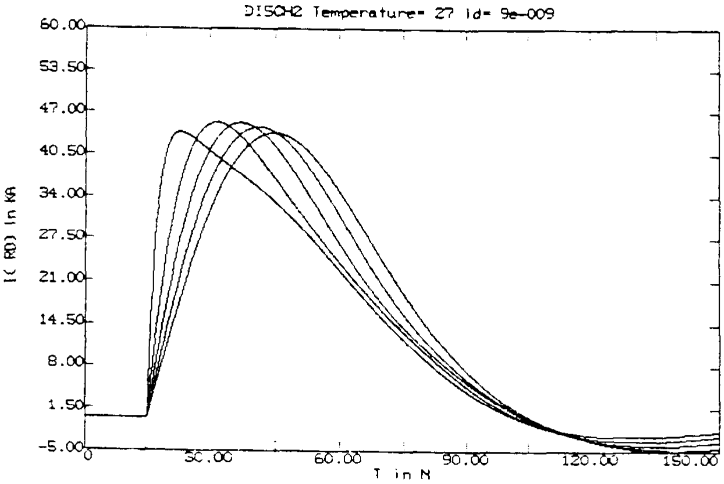

Figure 9. Typical current of discharge tube [I (RD)] as function of transient time (150 ns) for the different value of the tube inductance in the C-C circuit for 20 kV breakdown voltage. From top to bottom curves present variations for Ld = 1, 3, 5, 7, and 9 nH, respectively.

resulted which is decreased to about 1.2×10^{12} A/s for Ld = 9 nH. The result of this comparison leads to the fact that in order to have a high rate of current build up in the laser main discharge, the laser tube inductance should be as small as possible in operation. As can be seen in Figure 9 the nitrogen gas breakdown occurs at about 20 ns time delay which is governed by the discharge condition in the left hand charging loop.

The transient behavior of the C-C circuit is also studied for the various values of the laser tube resistance, Rd, in 150 ns time interval. The results of the laser discharge voltage and current are obtained for Rd = 0.15 to 0.55 Ω. The voltage variation is controlled by this parameter, and for example, for Rd = 0.15 Ω its risetime is 5.2×10^{11} V/s which would decrease to 3.3×10^{11} V/s for the tube resistance value of 0.55 Ω. The current analysis for this circuit is shown in Figure 10 which presents this variation for different discharge resistance values. The rate of the current increase is greatly controlled by this factor, whereas for Rd = 0.15 Ω the current risetime is about 3×10^{12} A/s in comparison to 2.1×10^{12} A/s for the Rd = 0.55 Ω. Another point of this computation is that the oscillatory behavior for current increases for lower Rd while increasing Rd value causes a quick damping

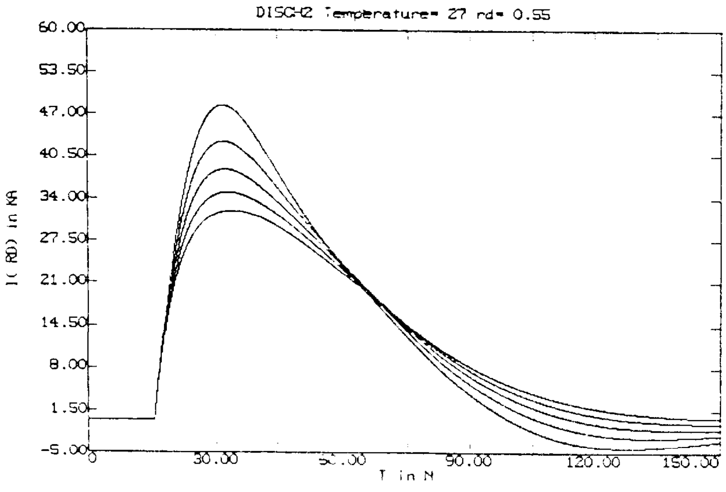

Figure 10. Transient behavior of the laser discharge current [I (RD)] for different plasma resistance, Rd, in the C-C circuit. From top to bottom are the curves for the Rd = 0.15, 0.25, 0.35, 0.45, and 0.55 Ω, respectively.

of the discharge current. However, the oscillation frequency is a little different for different Rd values as can be seen in Figure 10.

In a similar manner the transient behavior of the Blumlein discharge circuit is studied for the various values of the laser tube inductance and resistance. The result of voltage computation for variation of Ld from 1 to 9 nH is displayed in Figure 11. The general behavior of the voltage at the early stage of the gas breakdown is similar to that of the C-C circuit with two exceptions. The first is that the voltage breakdown occurs at about 15 ns time interval in comparison to 20 ns for the C-C circuit which shows that the Blumlein circuit is a faster excitation circuit. The second is that for the same Rd value the oscillatory behavior is the most pronounced of the Blumlein circuit.

Figure 12 shows the discharge current variations as a function of the tube inductance for the same assumed values, where this dependence for Ld=1 to 9 nH is investigated. All the current curves start from 15 ns time interval which indicate the gas breakdown in the main discharge for the same charging voltage. With an increase in the Ld, see Figure 12, the current peaks off more slowly which again shows the importance of the laser discharge inductance in current risetime. For this case at Ld=3nH, the current risetime is about 2.8×10^{12} A/s which is, relatively speaking, a good condition for a successful discharge operation. Another noticeable feature of this figure is that as the Ld value is increased the oscillatory behavior is enhanced, although at a time interval of about 150 ns all the curves reach zero value due to the damping factor.

The effect of the variation of Rd in this excitation circuit is also investigated at 150 ns discharge time. The dependence of tube load voltage is studied for R = 0.15 to 0.55 Ω and in this respect two points can be

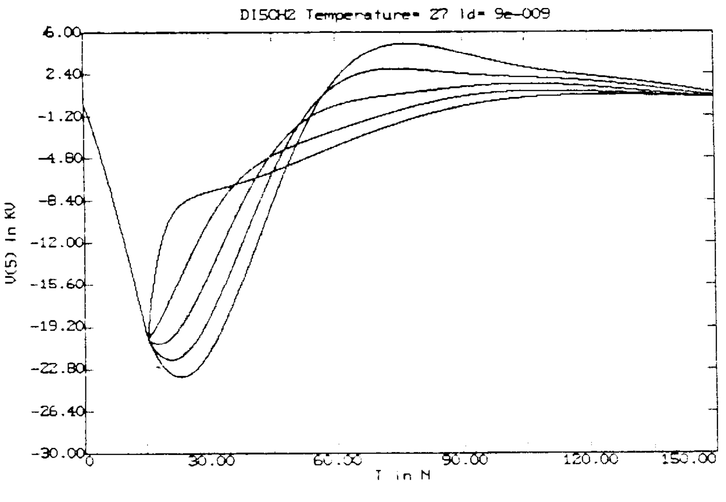

Figure 11. Time history of the laser load voltage [V (5)] for different tube inductance, Ld, for the Blumlein transmission line excitation and 20 kV breakdown voltage. From left to right are curves for Ld = 1, 3, 5, 7, and 9 nH, respectively.

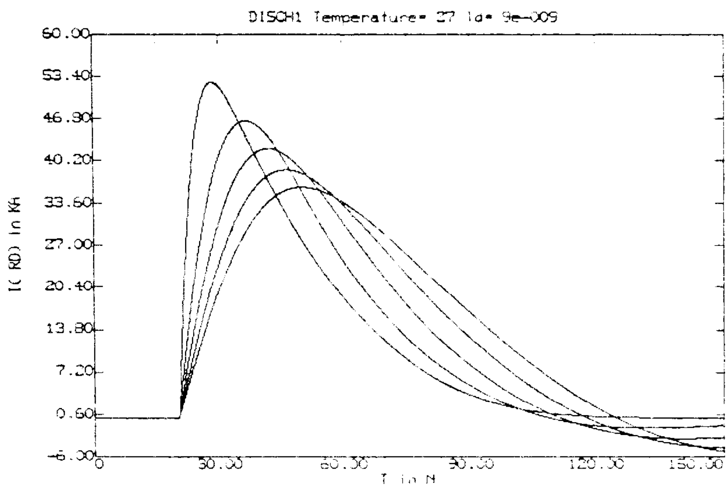

Figure 12. Typical time variation of the laser discharge current [I (RD)] with tube inductance, Ld, at fixed values of other parameters. From left to right different current curves correspond to L = 1, 3, 5, 7, and 9 nH, respectively (Blumlein).

the laser on time (150 ns) for different plasma resistance, Rd, in the Blumlein pulse generator. Different current curves from top to bottom present variations for Rd = 0.15, 0.25, 0.35, 0.45, and 0.55 Ω, respectively.

div., and for the lower traces is 10 kV/div. The horizontal scale for all traces is 10 ms/div., and the time interval which the input voltage goes through zero while the high voltage is maximum is identified by an arrow.